2021 International Seminar on Electron Devices Design and Production (SED)

Analysis of the Prospects for the Use of an Optical Displacement Sensor for Monitoring the Railroad Track

Vladimir Starostenko
School of computer engineering
HSE University
Moscow, Russia
vistarostenko@edu.hse.ru

Alexander Tuv
School of computer engineering
HSE University
Moscow, Russia
atuv@hse.ru

Sergei Polesskiy
School of computer engineering
HSE University
Moscow, Russia
spolessky@hse.ru

***Abstract*—This article studies the operation of an optical sensor with a cylindrical measured surface. Various options for positioning the sensor are considered. The study provides an estimation of the influence of the radius of the cylindrical reflective surface on the sensor transmission function.**

Keywords— infrared sensor, surface radius measurement

I. INTRODUCTION

Safety and reliability are fundamental requirements in the operation of railway systems. Among the issues of safety and reliability, ensuring the proper quality of the railroad track holds high priority.

One of the most important parameters to be monitored when diagnosing railway tracks is the compliance of the geometric proportions of the rail with the standard requirements. The normative values of the geometric parameters of the R-65 rail are shown in the figure 1.

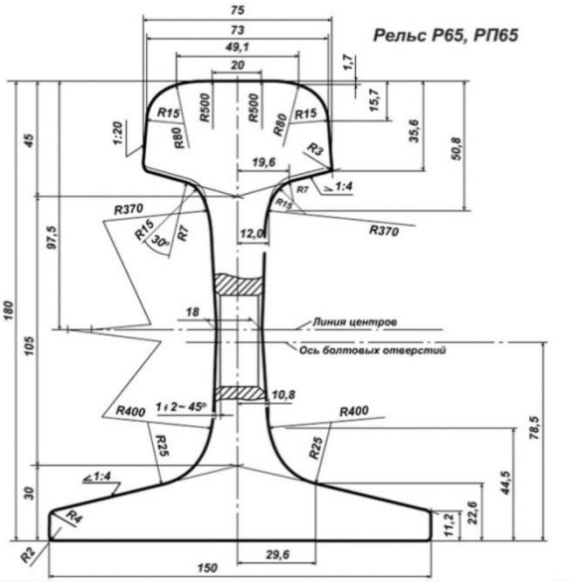

Fig. 1. Geometrical proportions of the P65 rail.

As portrayed in figure 1, one of the issues of rail quality check is assessing the degree of correspondence of rounded surfaces of various radius to the nominal values.

At present, in railway flaw detection, a profiler or devices based on the same principle are used to measure the geometric proportions of the track. The operation of the profiler is based on connecting the rail track with the needles on the device and transferring the resulting outline to paper or digital format. This method requires physical contact, which narrows the area of its applicability. In addition, measuring the characteristics of a rail using this method takes a significant amount of time, which, taking into account the length of the existing track to be monitored, is a disadvantage. Therefore, the issue of high-speed, non-contact measurements of the geometric proportions of rail tracks is of current interest. This article discusses the prospect of using an optical sensor to measure the radius of the rail surface.

II. METHODOLOGY FOR MEASURING

A reflectometric optical displacement sensor consists of a infrared source and a photodetector located in the same plane [1]. The sensor schematic is shown in Figure 2. The luminous flux from the infrared source is reflected by the surface and reaches the photodetector. The energy of the light flux entering the photodetector depends on the distance to the surface, the reflecting properties of the surface and the state of the environment in the gap between the reflecting surface and the source-receiver pair.

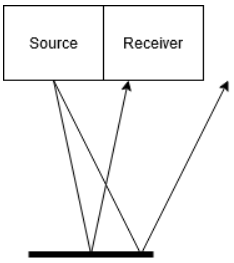

Fig. 2. Measurement scheme of an optical reflective sensor.

The model of a reflecting surface in the case of reflection from the rail track can be described by the composition of reflected light fluxes from flat and cylindrical surfaces. While the form and parameters of the transmission function for reflection from a flat surface are described in a number of works [2-16] and are well known, the issues of light flux

978-1-6654-3941-1 @2021 IEEE

reflection from the lateral surface of cylinders are practically not covered in the literature. This article studies the influence of the geometric parameters of cylindrical surfaces on the characteristics of an optical converter.

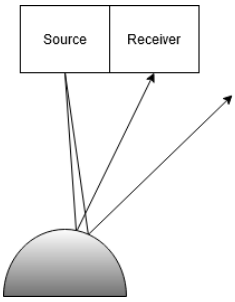

Fig. 3. Measurement scheme of an optical reflectometric sensor with a cylindrical reflecting surface.

III. Experiment

The aim of the study was to evaluate the influence of the surface radius on the output characteristics of the optical sensor. The schematic of the measuring device is shown in figure 4. The voltage across the photodiode was taken as The output characteristics were calculated using the photodiode voltage values gathered in a series of measurements with a set of variables. The distance from the sensor to the surface and the shift of the sensor perpendicular to the axis of the cylinder were chosen as the variable parameters. The location of the sensor relative to the surface also affects the transmission function of the device. In this article, two cases were studied: the axis connecting the source and receiver of the sensor located parallel to the cylinder axis and the axes located perpendicular to each other.

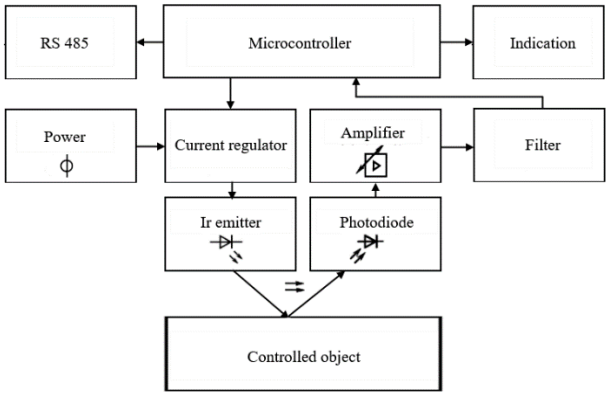

Fig. 4. Structural scheme of a reflectometric optical sensor.

The measurement scheme with the axes arranged parallel is shown in figure 5. The experiment consisted of two parts: measuring the influence vertical distance and horizontal shift have on the transmission function respectively.

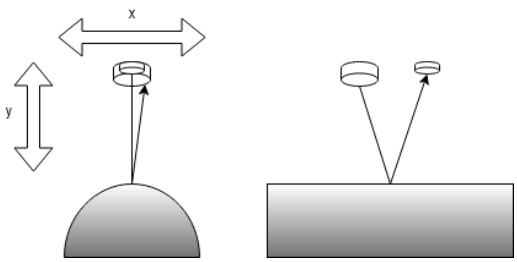

Fig. 5. Installation schematic of the sensor located parallel to the cylinder axis.

When measuring the influence of the vertical distance, the sensor was initially installed in the position, where it was touching the surface. Afterwards, the distance from the sensor to the surface was increased with a minimum step of 100 μm. The experiment was carried out on aluminum surfaces with a processing grade of 3-4 classes. The cylindrical surfaces had radii of 7.5, 15, 20 and 25 mm. The amount of measurement samples in a series depended on the shape of the output signal and was 61, 36, 42, and 53 for cylindrical surfaces, respectively, and 59 for a flat surface. The obtained data is presented in figure 6.

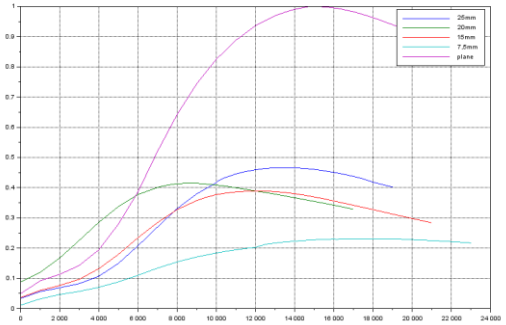

Fig. 6. Transmission function graphs for variable vertical distance and axes arranged parallel.

Optical converters have two points that determine the characteristics of the converter: the maximum point and the point, where the sensitivity of the converter is maximal. The maximum sensitivity was calculated using the obtained data for various cylinder radii.

TABLE I. Maximal sensitivity values with axes arranged parallel

Radius, mm	25	20	15	7.5
Sensitivity, relative units	6.76×10^{-5}	5.98×10^{-5}	5.51×10^{-5}	2.38×10^{-5}

Based on the data obtained, it was assumed that the sensitivity of the output signal, as well as the maximum value of the output voltage, directly correlates with the radius of the circle.

The next part of the study focused on the output characteristics of the sensor with a variable horizontal shift. In this experiment, the sensor was located at a distance corresponding to the operating point of the device. The operating point was defined as the point where the derivative of the output function is maximal. The initial position of the sensor was set so that the source-receiver axis would be directly above the cylinder axis. The experiment was carried out for surfaces with radii of 7.5, 15, 20 and 25 mm. The step was 2% of the surface radius, and the series included 51 samples. The obtained data is presented in figure 7.

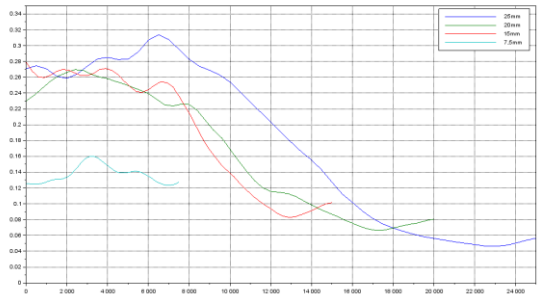

Fig. 7. Transmission function graphs for variable horizontal shift and axes arranged parallel.

Based on the results obtained, with a small horizontal shift, the data is hard to evaluate. Presumably, this is caused by surface roughness. Nevertheless, as the horizontal shift increases, the data takes on an organized form and has a corresponding shape, with a close to linear correlation between the minimum point and the surface radius.

TABLE II. MINIMAL OUTPUT POINT FOR VARIABLE HORIZONTAL SHIFT

Radius, mm	25	20	15	7.5
Minimum point, mm	23	17.2	12.9	6.9

The approximated function for the minimum point value is

$$x = 0{,}9 \cdot r - 0{,}32 \quad (1)$$

The last part of the experiment focused on the case, where the axis of the sensor was arranged perpendicular to the cylinder axis. The initial position of the sensor was set so that the photodiode would touch the surface. Then the distance from the surface was increased with a minimum step of 200 μm. The measurements were carried out for surfaces with radii of 7.5, 15, 20 and 25 mm. A series of measurements included 25 samples. The obtained data is presented in figure 9.

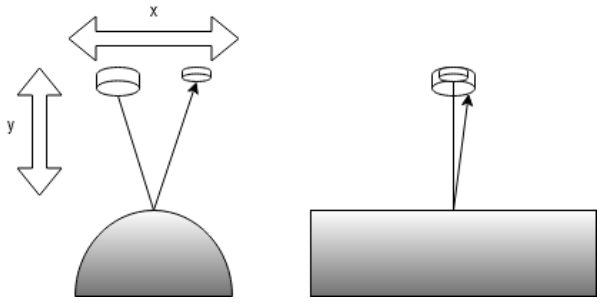

Fig. 8. Installation schematic of the sensor located perpendicular to the cylinder axis.

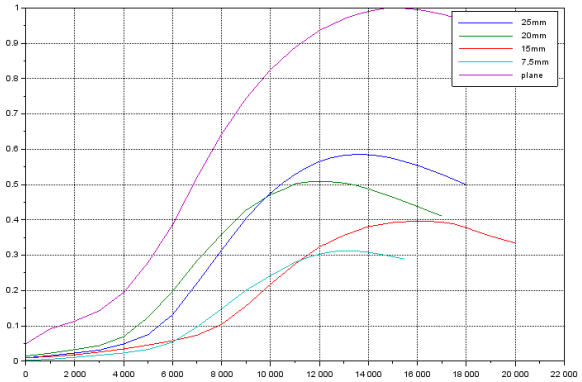

Fig. 9. Transmission function graphs for variable vertical distance and axes arranged perpendicular.

The data corresponds to the previously obtained for the parallel arrangement. Correlation between the sensitivity and the radius of the surface is similar to the one, observed in the previous parts of the experiment.

TABLE III. MAXIMAL SENSITIVITY VALUES WITH AXES ARRANGED PERPENDICULAR

Radius, mm	25	20	15	7.5
Sensitivity, relative units	9.32×10^{-5}	8.64×10^{-5}	6.12×10^{-5}	5.27×10^{-5}

IV. APPROXIMATION

For a more accurate description of the correlation between the output characteristics and the radius of the surface, a polynomial approximation of the output characteristics was carried out. The approximation was carried out for the full set of characteristics and for the area around the operating point for the vertical displacement measurements.

A fourth degree polynomial was used to approximate the full dataset. The resulting equations for the output function are listed in the table.

TABLE IV. APPROXIMATED FUNCTIONS FO COMPLETE DATASET

Surface	**Equation**
Flat surface	$u = 7.6 \cdot 10^{-2} - 4.2 \cdot 10^{-2} \cdot x + 2.6 \cdot 10^{-2} \cdot x^2 + +1.8 \cdot 10^{-3} \cdot x^3 + 3.6 \cdot 10^{-5} \cdot x^4$
R=25mm	$u = 5.4 \cdot 10^{-2} - 3.2 \cdot 10^{-2} \cdot x + 1.7 \cdot 10^{-2} \cdot x^2 + +1.2 \cdot 10^{-3} \cdot x^3 + 2.7 \cdot 10^{-5} \cdot x^4$
R=20mm	$u = 7.5 \cdot 10^{-2} + 5 \cdot 10^{-2} \cdot x + 3.2 \cdot 10^{-3} \cdot x^2 + +7.2 \cdot 10^{-4} \cdot x^3 + 2.4 \cdot 10^{-5} \cdot x^4$
R=15mm	$u = 3.8 \cdot 10^{-2} + 1.1 \cdot 10^{-2} \cdot x + 9.6 \cdot 10^{-3} \cdot x^2 + +8.3 \cdot 10^{-4} \cdot x^3 + 1.9 \cdot 10^{-5} \cdot x^4$
R=7.5mm	$u = 1.5 \cdot 10^{-4} + 9.4 \cdot 10^{-2} \cdot x + 2 \cdot 10^{-3} \cdot x^2 + +1.5 \cdot 10^{-4} \cdot x^3 + 2.9 \cdot 10^{-6} \cdot x^4$

For further calculations, the output function for a flat surface was set as standard, after which the deviation from the reference values for all obtained functions was calculated. The deviation was calculated by the formula

$$\frac{y_{standard} - y_{real}}{y_{standard}} \cdot 100\% \quad (2)$$

The values are presented in figure 10. The deviation from the standard is more than 40% for a surface radius of 25mm and more than 80% for a radius of 7.5mm. Thus, deviation can be used to assess the similarity of the state of the surface

with the reference state of a flat surface. However, some values of the radius cannot be distinguished from each other, as can be seen from the example of deviations for a radius of 15 and 20 mm.

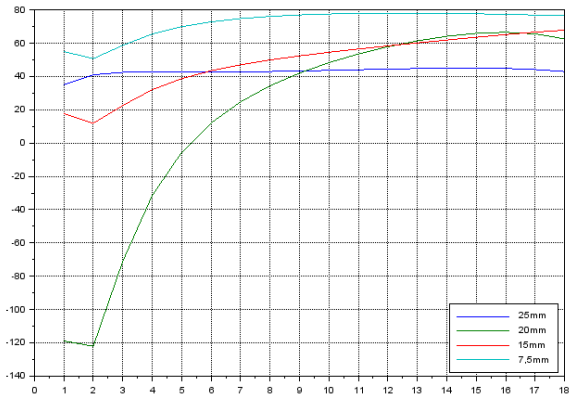

Fig. 10. Output characteristics deviation from reference values.

Next, the data were approximated in the working area. Since the data around the operating point has a form close to linear, the approximation was performed for a linear function. First, the data was processed for the case of parallel arrangement. The resulting equations are listed in the table.

TABLE V. APPROXIMATED FUNCTIONS WITH AXES ARRANGED PARALLEL

Radius, mm	function
25	$u = 5.46 \cdot 10^{-5}x - 1.17 \cdot 10^{-1}$
20	$u = 4.38 \cdot 10^{-5}x + 7.8 \cdot 10^{-2}$
15	$u = 3.37 \cdot 10^{-5}x + 8 \cdot 10^{-3}$
7.5	$u = 1.70 \cdot 10^{-5}x + 9 \cdot 10^{-3}$

According to the equations, the correlation between the first coefficient of the function and the surface radius is close to linear (fig. 11).

$$k = 22 \cdot 10^{-6}r + 8 \cdot 10^{-6} \quad (3)$$

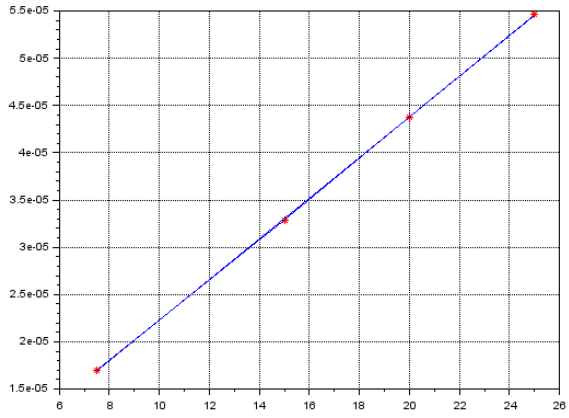

Fig. 11. Linear approximation of the first coefficient value with parallel axis arrangement.

Further, similar calculations were carried out for the perpendicular arrangement of the sensor. The resulting equations are listed in the table.

TABLE VI. APPROXIMATED FUNCTIONS WITH AXES ARRANGED PERPENDICULAR

Radius, mm	function
25	$u = 8.73 \cdot 10^{-5}x - 0.388$
20	$u = 7.90 \cdot 10^{-5}x - 0.272$
15	$u = 5.59 \cdot 10^{-5}x - 0.344$
7.5	$u = 4.60 \cdot 10^{-5}x - 0.220$

In this case, the correlation between the coefficient and the radius is less linear, as shown in figure 12. The resulting approximated equation for the coefficient is

$$k = 25 \cdot 10^{-6}r + 2.46 \cdot 10^{-4} \quad (4)$$

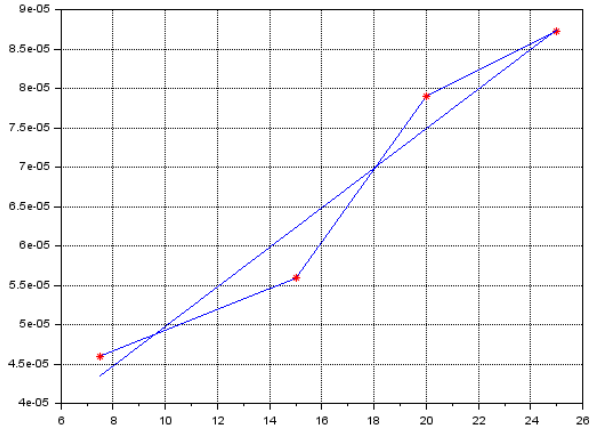

Fig. 12. Linear approximation of the first coefficient value with perpendicular axis arrangement.

CONCLUSION

According to the performed analysis of the correlation between the radius of the cylindrical reflection surface and the output function of the optical reflective sensor, various output characteristics can be used to asses the rail track defects. Based on the approximated functions, it was concluded that surface curvature can be determined based on the deviation of the output characteristics from the reference values. However, this method is not always able to distinguish between different surface parameters. More accurate results can be obtained from sensitivity analysis in the operating area of the output function. With a variable vertical distance, the correlation between the sensitivity and the surface radius was close to linear. Out of the two considered options for the location of the sensor, the closer to linear results were obtained with a parallel arrangement of the sensor and cylinder axes. In this case, the transmission function for the sensitivity coefficient was approximated to the equation 3.

With a variable horizontal shift, the output characteristics correlated less with the surface radius. However, by positioning the sensor parallel to the cylinder axis, it is possible to estimate the surface radius based on the minimum point of the function. The approximate function for the minimum point value is shown in equation 1.

According to the results of the studies, the sensor using vertical displacement allows more accurate assessment of the track defects. However this method limits the speed of data gathering, since the sensor needs to stop at the evaluated point to gather the data at different vertical positions one at a time. Considering that the data with lower accuracy can be sufficient during the rail track check, the sensor with a horizontal shift can show better result. The issue with the time taken to gather the data at a sertain point of the track can be resolved by using multiple photodiodes instead of shifting one. The schematic of the measuring device is presented in figure 13, where the sensor consisting of photodiodes and light sources is marked 1 and the rail track profile is marked 2.

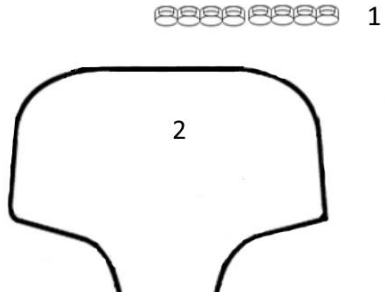

Fig. 13. Measurement scheme of an optical reflectometric sensor with eight phtodiodes.

REFERENCES

[1] Zak E.A. Volokonno-opticheskie preobrazovateli s vneshnej moduljaciej [Fiber optic transducers with external modulation]. Moscow. Energoatomizdat Publ., 1989. - 128 p.

[2] Dmitriyev A.V., Krasivskaya M.I., Yurin A.I. Study of fiber optic sensors with external modulation. Datchiki i Sistemy [Sensors and Systems], 2013, no. 5, p.p. 34 - 37.

[3] GOCT 28205. Basic environmental testing procedures. Part 2. Tests. Guidance for solar radiation testing. (In Russian). https://internet-law.ru/gosts/gost/2971/ (as of March 30, 2020).

[4] Miroshnichenko I.P. Advanced device for measuring linear and angular components of small displacements of monitor object surfaces [Perspektivnoe ustroystvo dlya izmereniya lineynykh i uglovykh sostavlyayushchikh malykh peremeshcheniy poverkhnostey ob"ekta kontrolya]. Vestnik Donskogo gosudarstvennogo universiteta [Bulletin of the Don State University], 2017, no.1, pp.55-66.(In Russian).

[5] Jianjun Pan, Qiuming Nan, Shujie Li, Zhonghua Hao, Development of a high resolution optical-fiber tilt sensor by F-P filter. Proceedings of 25th International Conference on Optical Fiber Sensors, 2017, DOI: 10.1117/12.2265964.

[6] Mao-qing Chen, Yong Zhao, Ri-qing Lv, Feng Xia, A novel and small curvature sensor based on butterfly-shape Mach-Zehnder interferometer, Proceedings 25th International Conference on Optical Fiber Sensors, 2017, DOI 10.1117/12.2262331

[7] Mikhaylov M.A., Manoylov V.V. The overview of measure methods of slight displacements in the application of the automatic regulation system of scanners of scanning probe microscopes [Obzor metodov izmereniya malykh peremeshcheniy v prilozhenii sistemy avtomaticheskogo regulirovaniya skanerov SZM], Nauchnoe priborostroenie [Scientific instrument engineering], 2013, i.23, no.2, pp.27-37.(In Russian).

[8] Shishkin V.V., Granev I.V., Shelemba I.S. Domestic experience in production and application of fiber optic sensors [Otechestvennyy opyt proizvodstva i primeneniya volokonno-opticheskikh datchikov], Prikladnaya fotonika [Applied photonics], 2016, i.,no.1, pp. 61-75.(In Russian).

[9] García I., Zubia J., Berganza A., Beloki J,, Arrue J., Illarramendi M.A., Mateo J., Vázquez C., Different Configurations of a Reflective Intensity-Modulated Optical Sensor to Avoid Modal Noise in Tip-Clearance Measurements, Journal of Lightwave Technology, 2015, vol.33 , i.12, DOI: 10.1109/JLT.2015.2397473

[10] Perrone G., Vallan A., A Low-Cost Optical Sensor for Noncontact Vibration Measurements, IEEE Transactions on Instrumentation and Measurement, 2009, vol.58 , I. 5, DOI: 10.1109/TIM.2008.2009144.

[11] Wenwei Zheng, Yuhua Wang, Xiang Cheng, Zhiting Liu, A non-contact dynamic angular displacement detecting method for detecting the sheet metal structure of household appliance, Proceedings of the 29th Chinese Control and Decision Conference (2017CCDC). DOI: 10.1109/CCDC.2017.7978589

[12] Y. I. Gudkov, V. N. Azarov and A. L. Tuv, "Active infrared sensor for monitoring protected areas," *2017 International Conference "Quality Management,Transport and Information Security, Information Technologies" (IT&QM&IS)*, St. Petersburg, 2017, pp. 725-727, doi: 10.1109/ITMQIS.2017.8085927.

[14] Y. I. Gudkov, V. N. Azarov and A. L. Tuv, "Fiber optic sensor for monitoring vibration load," 2016 IEEE Conference on Quality Management, Transport and Information Security, Information Technologies (IT&MQ&IS), Nalchik, Russia, 2016, pp. 57-60, doi: 10.1109/ITMQIS.2016.7751901.

[15] A. L. Tuv and Y. I. Gudkov, "Adaptive Measuring System for On-line Monitoring of Parameters of Radio-electronic Means," 2019 International Conference "Quality Management, Transport and Information Security, Information Technologies" (IT&QM&IS), Sochi, Russia, 2019, pp. 316-319, doi: 10.1109/ITQMIS.2019.8928451.

[16] M. S. Akatov, S. N. Safonov and A. L. Tuv, "Analysis of Parameters of Optical Linear Displacement Transducer with Open Channel," 2020 International Conference Quality Management, Transport and Information Security, Information Technologies (IT&QM&IS), Yaroslavl, Russia, 2020, pp. 170-172, doi: 10.1109/ITQMIS51053.2020.9322872.